Research Article

Journal of PeptideScience

Received: 15 April 2009 Revised: 14 June 2009 Accepted: 16 June 2009 Published online in Wiley Interscience: 18 August 2009

(www.interscience.com) DOI 10.1002/psc.1162

Preliminary studies on noncovalent hyperbranched polymers based on PNA and DNA building blocks

Maria Moccia,[a] Domenica Musumeci,[a]* Giovanni N. Roviello,[a] Sabato Fusco,[b] Margherita Valente,[a] Enrico M. Bucci,[a] Roberto Sapio,[a] Carlo Pedone[a] and Paolo A. Netti[b]

In this work, we report thermodynamic, kinetic, and microrheological studies relative to the formation of PNA- and PNA/DNA-based noncovalent polymeric systems, useful tools for biotechnological and bioengineering applications. We realized two kinds of systems: a PNA-based system formed by a self-assembling PNA tridendron, and a PNA/DNA hybrid system formed by a PNA tridendron and a DNA linker. The formation of a three-dimensional polymeric network, by means of specific Watson–Crick base pairing, was investigated by a detailed UV and CD spectroscopic study. Preliminary microrheology experiments were performed on both systems to evaluate their viscoelastic properties which resulted in agreement with the formation of soluble hyperbranched polymers that could be useful for drug/gene delivery, as well as for encapsulating organic pollutants of different shapes and sizes in environmental applications.

Keywords: noncovalent polymers; PNA/DNA building blocks; UV/CD studies; microrheology

Introduction

Dendrimers are a class of highly branched synthetic macromolecules suitable for a wide variety of biomedical and bioengineering applications [1–3], ranging from drug delivery [4,5], imaging [6], or cell transfection [7], to the development of new tools for the removal of pollutants from water [8], as well as innovative materials for electronic or optical devices [9].

By taking advantage of the nucleobase recognition, based on Watson–Crick (W-C) hydrogen bonding, many researchers investigated dendrimeric self-assembling systems based on DNA [10] to realize new nanomaterials [11,12] with enhanced functionality, as well as hydrogels to be used as drug/gene delivery systems [13] or as tissue engineering scaffolds [14]. The control of the reversible aggregation/disaggregation of such systems is an intriguing goal especially in the drug delivery field. This aim could be achieved, for example, by the conjugation of DNAs to metal nanoparticles sensitive to external stimuli, as in the case of the remote electronic control over the hybridization properties of an Au–DNA nanoconjugate upon exposure to radio frequency magnetic fields [15].

Herein, we report the design, synthesis, and chemical and physical characterization of two dendrimeric systems, one based uniquely on PNA [16] (homocomplex system **A**, Figure 1a) and the other one based on PNA and DNA building blocks (hybrid system **B**, Figure 1a). Both systems are expected to possess the ability to form, by means of specific W-C base pairing, a three-dimensional polymeric network sensitive to temperature, or other external factors, to be used as drug/gene delivery tools or for the removal of pollutants from water. We studied the thermodynamic, kinetic, and microrheological behavior of these systems to verify the optimal conditions for network formation. The presence of PNAs in this kind of systems should increase thermal and enzymatic stability of the entire structure, and reduce the immune response induced by systems made entirely from DNA, desirable aspects in view of their future *in vivo* applications.

Materials and Methods

Chemicals

Fmoc–Gly–OH, HATU, Fmoc–Lys(Boc)–OH, Fmoc–Lys (Fmoc)–OH, and PyBOP were purchased from Novabiochem. Anhydroscan DMF and NMP were purchased from LabScan. Piperidine was from Biosolve. Solvents for HPLC chromatography and acetic anhydride were from Reidel-de Haën. TFA and Rink-amide resin were from Fluka. PNA kit, of Perspective Biosystem, consists of

* *Correspondence to: Domenica Musumeci, Istituto di Biostrutture e Bioimmagini – CNR, via Mezzocannone 16, 80134 Naples, Italy.*
E-mail: domymusu@alice.it

a *Istituto di Biostrutture e Bioimmagini – CNR, via Mezzocannone 16, 80134 Naples, Italy*

b *Dipartimento di Ingegneria dei Materiali e della Produzione, Università "Federico II", Piazzale Tecchio 80, 80125 Naples, Italy*

Abbreviations used: *Bhoc, benzhydryloxycarbonyl; Boc, tert-butoxycarbonyl; CD, circular dichroism; DIEA, N,N-diisopropylethylamine; DMF, N,N-dimethylformamide; Fmoc, 9-fluorenylmethoxycarbonyl; HATU, O-(7-azabenzotriazol-1-yl)-N,N,N′,N′-tetramethyluronium hexafluorophosphate; NMP, 4-methylpyrrolidone; PTFE, polytetrafluoroethylene; PyBOP, (1H-benzotriazol-1-yloxy) tripyrrolidinophosphonium hexafluorophosphate; RP, reverse phase; TFA, trifluoroacetic acid; MPT, multiple particle tracking; MSD, mean square displacement; NMP, 4-methylpyrrolidone; PTFE, polytetrafluoroethylene.*

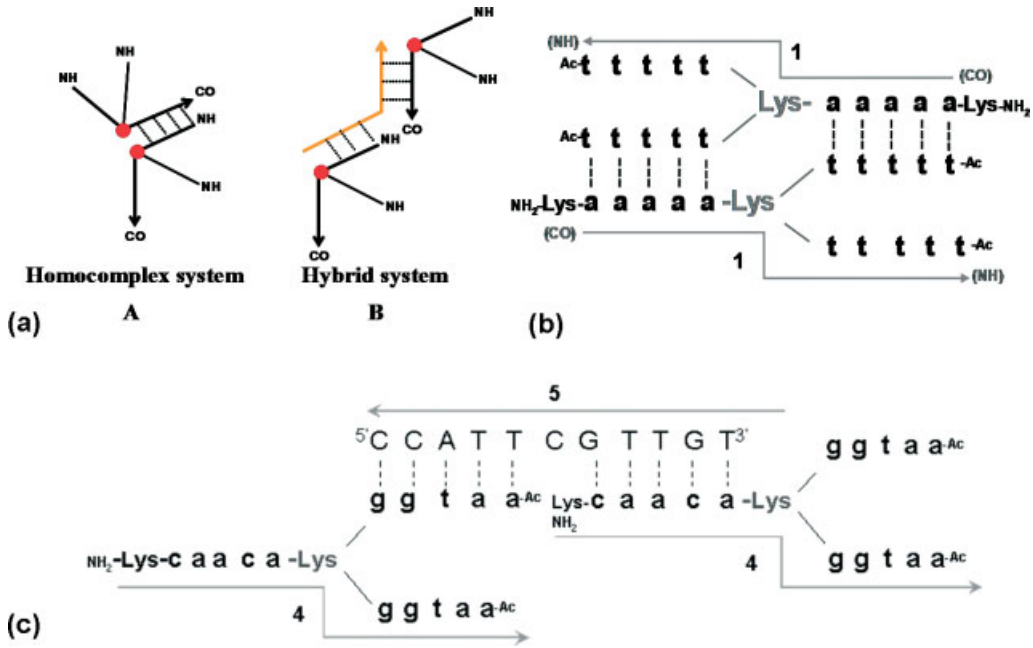

Figure 1. (a) Schematic view of noncovalent polymeric systems **A** and **B**; (b) system **A** formed by PNA **1**; and (c) system **B** formed by PNA **4** and DNA **5**.

the following: Fmoc/Bhoc PNA monomers, HATU activator, base solution (0.2 M DIEA, 0.3 M lutidine), Wash B (anhydrous DMF), capping solution (5% Ac_2O, 6% 2,6-lutidine in DMF), deblock solution (20% piperidine in DMF). TFA (for HPLC) were from Romil.

Apparatus

Automatic synthesizer for DNA/PNA synthesis was Applied Biosystems Expedite 8909. Centrifugations were performed using Z 200 A Hermle centrifuge. Products were analyzed and characterized by LC-MS, performed on an MSQ mass spectrometer (ThermoElectron, Milan, Italy) equipped with an ESI source operating at 3 kV needle voltage and 320 °C, and with a complete Surveyor HPLC system, comprising a MS pump, an autosampler, and a PDA detector, by using a Phenomenex Jupiter C18 300 Å (5 µm, 4.6 mm × 150 mm) column. Gradient elution was performed at 40 °C (monitoring at 260 nm) by building up a gradient starting with H_2O (0.05% TFA) and applying acetonitrile (0.05% TFA) with a flow rate of 0.8 ml/min. MALDI-TOF MS spectra were obtained on a PerSeptive Biosystems Voyager-DE MALDI-TOF mass spectrometer using, as matrix, 8 : 1 3-hydroxypicolinic acid/ammonium citrate in 1 : 1 water/acetonitrile (negative mode). Semi-preparative purifications of PNA and DNA were performed by HPLC on a Hewlett Packard/Agilent 1100 series instrument, equipped with a diode array detector. PNA separation was achieved by using a Phenomenex Juppiter C18 300 Å (10 µm, 10 mm × 250 mm) column at 45 °C (monitoring at 260 nm), building up a gradient starting with buffer A (0.1% TFA in water) and applying buffer B (0.1% TFA in acetonitrile) with a flow rate of 4 ml/min. DNA separation was performed by using an anion exchange analytical column (Nucleogel SAX, Machery Nagel, 4.6 mm × 50 mm) applying a linear gradient of B_1 in A_1, where solvent A_1 was made up of 20 mM K_2HPO_4, pH 7.0, 20% CH_3CN, and B_1 of 1 M KCl in 20 mM K_2HPO_4, pH 7.0, 20% CH_3CN (flow rate 1 ml/min). HPLC detection was achieved at 260 nm. PNA and DNA samples were lyophilized in a FD4 freeze dryer (Heto Lab Equipment) for 16 h. CD spectra were obtained on a Jasco J-810 spectropolarimeter. UV spectra and UV melting experiments were recorded on a Jasco V-550 UV–Vis spectrophotometer equipped with a Peltier ETC-505T temperature controller. Microrheology experiments were performed on an Olympus 1 × 51 microscope (×10, ×60, ×100 lenses) equipped with an Hg lamp and a camera Princeton Instrumentation Micromax 5 MHz (model vt-133).

Synthesis and Characterization of PNAs 1–4

The PNA sequences are (Ac-t-t-t-t-t)$_2$-K-a-a-a-a-a-K-NH_2 (**1**), H-G-a_5-K-NH_2 (**2**), H-G-t_5-KK-NH_2 (**3**); (Ac-a-a-t-g-g)$_2$-K-a-c-a-a-c-K-NH_2 (**4**).

Solid support functionalization and manual solid-phase oligomerizations were carried out in short SPP columns (4 ml) equipped with a PTFE filter, a stopcock, and a cap. Solid support used was Rink-amide resin (0.5 mmol NH_2/g). The Rink-amide resin (160 mg, 80 µmol) was functionalized with a lysine (Fmoc-Lys(Boc)-OH, 18.7 mg, 40 µmol, 0.5 eq) using PyBOP (20.8 mg, 40 µmol, 0.5 eq) as activating agent and DIEA (13.6 µl, 80 µmol, 1 eq) as base for 30 min at room temperature. Capping of the unreacted amino groups on the resin was performed with Ac_2O (20%)/DIEA (5%) in DMF. The loading of the resin was checked by measuring the absorbance of the released Fmoc group ($\varepsilon_{301} = 7800$) after treatment with a solution of piperidine (30%) in DMF (UV Fmoc test) and was found to be reduced to 0.25 mmol/g compared to the initial functionalization (almost quantitative yield with respect to the Fmoc-Lys(Boc)-OH used). A further Fmoc-Lys(Boc)-OH was analogously added for the synthesis of oligomer **3**: also in this case the reaction yield was quantitative (UV Fmoc test). Automatic solid-phase assembly of the PNAs was performed using Fmoc chemistry and a standard 2 µmol scale protocol, unless otherwise specified, and the final Fmoc group was left on the resin to evaluate, by the UV Fmoc test, the overall synthetic yield. After manual removal and quantification of the final Fmoc group, **1** and **4** were acetylated (5% Ac_2O, 6% lutidine in DMF) on their *N*-termini, whereas a glycine residue (3 eq) was attached manually to the *N*-termini of the oligomers **2** and **3** by using PyBOP

(3 eq)/DIEA (6 eq) as activating system in DMF. Successively, all oligomers were cleaved from the resin and deprotected under acidic conditions (TFA/*m*-cresol, 4 : 1 v/v). The crude oligomers were isolated by precipitation with cold diethyl ether, centrifugation, and lyophilization. Purified oligomers (semi-preparative HPLC) were characterized by LC-ESI-MS and quantified by UV measurements. Absorbance at $\lambda = 260$ nm of PNA solutions was measured at 85 °C, and extinction coefficients (ε_{260}) of the PNA monomers used for the quantification were 13 700 (a), 6600 (c), 11 700 (g), 8600 (t) M^{-1} cm^{-1}.

$(Ac\text{-}t_5)_2$-K-a_5-K-NH_2 (**1**). The first poly adenine tract of **1** was assembled by the automatic synthesizer on Rink-amide-K-NH_2 resin (4 μmol). Successively, a Fmoc-Lys(Fmoc)-OH (32 μmol, 8 eq) was manually added using HATU (28.8 μmol, 7.2 eq) and base solution (160 μl), performing a double coupling (15 min each). The simultaneous removal of the two Fmoc groups on the central lysine allowed both thymine branches to grow on the automatic synthesizer, using a modified protocol with a double coupling. Final UV Fmoc test provided a 24% overall yield. The cleaved and deprotected oligomer was purified by semi-preparative RP-HPLC using a linear gradient of 10% (for 5 min) to 20% B in A over 35 min: $t_R = 27.7$ min. UV quantification provided 395 nmol (1.7 mg) of the purified oligomer **1** ($\varepsilon_{260} = 154\,500$ M^{-1} cm^{-1}). ESI-MS *m/z*: 1463.85 (found), 1466.33 (expected for $[M + 3H]^{3+}$); 1097.88 (found), 1099.75 (expected for $[M + 4H]^{4+}$).

H-G-a_5-K-NH_2 (**2**) was assembled automatically on Rink-amide-K-NH_2 resin. Final UV Fmoc test furnished a 37% overall yield. The oligomer was purified by semi-preparative RP-HPLC using a linear gradient of 1% (for 5 min) to 18% B in A over 30 min: $t_R = 20.2$ min. UV quantification provided 880 nmol (1.4 mg) of the purified oligomer **2** ($\varepsilon_{260} = 68\,500$ M^{-1} cm^{-1}). ESI-MS *m/z*: 526.57 (found), 526.72(expected for $[M + 3H]^{3+}$); 790.38 (found), 789.58 (expected for $[M + 2H]^{2+}$).

H-G-t_5-KK-NH_2 (**3**) was obtained automatically on Rink-amide-KK-NH_2 resin. Final UV Fmoc test furnished a 33% overall yield. RP-HPLC purification was performed using a linear gradient of 5% (for 5 min) to 22% B in A over 30 min: $t_R = 26.8$ min. UV quantification provided 720 nmol (1.2 mg) of the purified oligomer **3** ($\varepsilon_{260} = 43\,000$ M^{-1} cm^{-1}). ESI-MS *m/z*: 831.8 (found), 831.76 (expected for $[M + 2H]^{2+}$); 1661.8 (found), 1661.64 (expected for $[M + H]^{+}$).

$(Ac\text{-}a\text{-}a\text{-}t\text{-}g\text{-}g)_2$-K-a-c-a-a-c-K-$NH_2$ (**4**) was obtained analogously to **1**. Final UV Fmoc test furnished a 25% overall yield. PNA **4** was purified by semi-preparative RP-HPLC using a linear gradient of 8% (for 5 min) to 18% B in A over 35 min: $t_R = 24.4$ min. UV quantification provided 400 nmol (1.8 mg) of the purified oligomer **4** ($\varepsilon_{260} = 173\,100$ M^{-1} cm^{-1}). ESI-MS *m/z*: 1021.15 (found), 1122.2 (expected for $[M + 4H]^{4+}$); 1494.06 (found), 1492.97 (expected for $[M + 3H]^{3+}$).

Synthesis and Characterization of DNA 5

The synthesis of oligonucleotide **5** (C-C-A-T-T-C-G-T-T-C-T) was performed on automatic synthesizer using standard phosphoramidite chemistry and 1 μmol scale protocol. DNA synthesis was carried out in 3′ to 5′ direction using, as solid support, CPG 500 Å resin (40 μmol/g, 1 μmol), functionalized with the first 3′-hydroxyl-5′-dimethoxytrityl-nucleoside. After deprotection and cleavage from the solid support with ammonia solution (55 °C, 15 h), the crude oligomer was purified by HPLC and desalted by gel filtration on a NAP-25 column. Desalted oligomer was characterized by MALDI-TOF (*m/z*: 3294, found; 3299, expected for MH^-) and quantified by UV. UV quantification of **5** was performed by measuring the A_{260} at 85 °C, using the $\varepsilon_{260} = 104\,700$ M^{-1} cm^{-1}, calculated considering as extinction coefficients for the single bases the following values: 15 400 (A), 7300 (C), 11 700 (G), 8800 (T) M^{-1} cm^{-1}. In this way, 586 nmol (1.9 mg, 58.6% yield) of purified product was estimated.

UV and CD Studies

Annealing of the PNA/DNA strands was performed by dissolving the oligomers in H_2O (pH 7.0), heating the solutions at 85 °C (5 min), allowing to cool slowly to room temperature and then keeping overnight at 4 °C. UV and CD measurements were performed in Hellma quartz Suprasil cells, with a light path of 1 cm and 2 × 0.4375 cm (tandem cell). Thermal melting curves were obtained in a 1-cm cell by recording the UV absorbance at 260 nm while the temperature was increased at 0.5 °C/min. T_m values were calculated by the first derivative method. CD spectra were recorded from 320 to 200 nm in H_2O (pH 7.0) at 20 °C: scan speed 50 nm/min, data pitch 2 nm, band width 2 nm, response 4 s, three accumulations.

CD binding experiment on oligomers **4** and **5** was performed as follows: first, 1-ml solutions in H_2O of PNA tridendron **4** (4 μM) and DNA **5** (10 μM) were kept each in one of the tandem cell reservoirs and the CD spectrum from 200 to 320 nm, corresponding to the *sum* spectrum of the separated strands, was registered. Successively, the cell was turned upside down to allow the mixing of the two samples and again a CD spectrum, corresponding to the *mix*, was recorded.

Kinetic CD experiment on system **B** was performed by recording the CD signal, at 240 and 275 nm, immediately after the mixing of **4** and **5** in the tandem cell, at the following times: 1, 8, 16, 24, 36, 44, 53, 61, 70, 73, 115, 150, 215, 300 min.

Microrheology Experiments

Samples of systems **A** and **B** were prepared for microrheology experiments by dissolving the lyophilized oligomers in 200 μl of water at pH 7.0, heating at 90 °C for 5 min, slowly cooling at room temperature, and finally storing at 4 °C for 12 h. The mixtures were embedded with 3 μl of diluted solution of fluorescent polystyrene beads (0.55 μm). The beads are molecular probe with 0.2% of the solid part in solution. Eighty microliters of each sample was fixed in a chamber on glass slides to perform microrheology experiments at microscope. For system **A**, the tests were performed using 50 and 200 μM concentrations at 20 °C. For system **B**, we used the optimal tridendron/linker ratio (1 : 2), and 50 and 200 μM overall concentrations at 20 °C.

Results and Discussion

PNA-based Noncovalent Polymer

The homocomplex system **A** is formed by the PNA tridendron **1** (Figure 1b) having the following self-complementary sequence: $(Ac\text{-}t\text{-}t\text{-}t\text{-}t\text{-}t)_2$-K-a-a-a-a-a-$KNH_2$. PNA **1** was assembled on an automatic synthesizer using 2 μmol scale standard protocol and Fmoc chemistry. Starting from the *C*-terminus, **1** is constituted by an L-lysine residue, a penta-adenine branch (a_5), an additional L-lysine in the middle of the sequence, and two penta-thymine branches (t_5), assembled simultaneously on both amino groups of the central lysine that was doubly Fmoc-protected. The

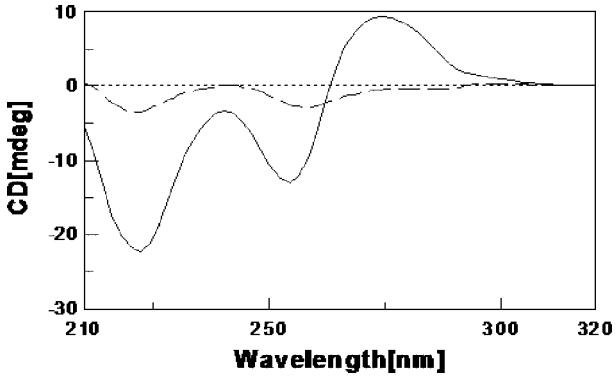

Figure 2. CD spectra of the PNA tridendron **1** (solid line) and of the a_5/t_5 (**2**/**3**) 1 : 1 complex (dashed line), 8 μM concentration in H_2O, pH 7.0, 20 °C.

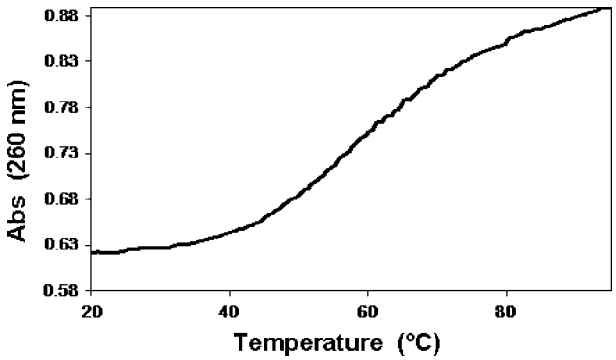

Figure 3. UV melting of the PNA tridendron **1** (4 μM in H_2O, pH 7.0).

C-terminal lysine was useful to improve the final product solubility [17]. After removal and quantification of the final Fmoc groups (24% overall yield), the oligomer was acetylated on both *N*-termini and cleaved/deprotected by acidic treatment. PNA tridendron was purified by RP-HPLC (10% yield) and characterized by LC-ESI-MS.

CD spectrum of the annealed PNA **1** is shown in Figure 2 (solid line) and revealed the presence of two main bands: one positive with a maximum at 275 nm, and the other negative with a maximum at 240 nm. The evidence of this distinct CD signal is indicative of multiple H-bonds formation: indeed, PNAs, while do not show a significant CD signal as single strands, however, exhibit a clear CD when they form duplex or triplex structures. Furthermore, the intensity of the CD bands for **1** is rather strong if compared with that of homoadenine/homothymine PNA/PNA complexes that show only a weak CD signal, as reported in literature [18,19]. Therefore, in the case of PNA **1**, composed of penta-adenine/penta-thymine tracts, the strong CD signal could be associated with the formation of a multimeric network based on PNA–tridendron complexes.

On the basis of comparison of the CD spectrum of Figure 2 (solid line) with literature data, we propose the formation of PNA/PNA double helices [18] with a dominating left-handed helicity [20,21] as components of the supramolecular network.

UV thermal denaturation of the polymeric system based on the self-assembling PNA **1** furnished a T_m of 58 °C at 4 μM concentration (Figure 3). Interestingly, only one transition was detected, according to the presence of duplex structures at the basis of the supramolecular system. The process was reversible and the pairings were completed in about 45 °C (90 min at 0.5 °C/min).

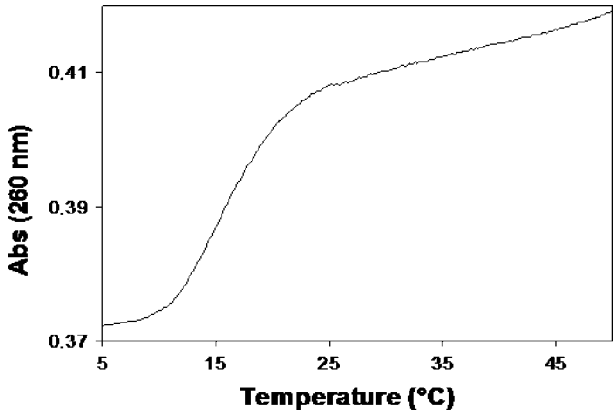

Figure 4. UV melting curve of the 4 μM a_5 (**2**)/t_5 (**3**) 1 : 1 complex in H_2O, pH 7.0.

In order to support the formation of a supramolecular network for the three-branched PNA **1**, we synthesized, as controls, two linear PNA strands having the sequences of the PNA tridendron arms: H-G-a_5-KNH$_2$ (**2**) and H-G-t_5-KKNH$_2$ (**3**). The UV melting curve of the 1 : 1 **2**/**3** complex showed a T_m value of only 19 °C at 4 μM concentration (Figure 4) in comparison to 58 °C for tridendron **1** at the same concentration, demonstrating that the lysine core in PNA **1** does not interrupt significantly the continuity of the duplexes. The denaturation process was reversible, and the pairings were completed in about 12 °C (24 min at 0.5 °C/min) denoting a high degree of co-operativity, in contrast to PNA **1** (Figure 3). Furthermore, the CD spectrum of the a_5/t_5 complex (Figure 2, dashed line) showed weaker bands than that of PNA tridendron **1** and was reminiscent of a triplex structure, not formed in case of PNA tridendron **1** probably because of the steric hindrance of the noncovalent polymeric network.

PNA/DNA-based Noncovalent Polymer

Because the extension of the one-component system **A** is not easily controllable, without acting on the concentration of PNA **1**, we also designed and realized a system having two different building blocks (**B**, Figure 1a). This two-component system is composed of a 15-mer PNA tridendron with a non-self-complementary sequence (**4**) and a DNA linker (**5**, Figure 1c) with a sequence complementary to five-base tracts of the PNA tridendron: in this way two PNA molecules are linked together by one DNA linker *via* hydrogen bonds allowing the formation of a three-dimensional network of PNA/DNA duplexes.

The PNA sequence is (Ac-a-a-t-g-g)$_2$-K-a-c-a-a-c-KNH$_2$ (**4**), whereas the DNA sequence is C-C-A-T-T-C-G-T-T-C-T (**5**). PNA **4** was synthesized on solid phase by using Fmoc chemistry and 2 μmol scale standard protocol. The crude PNA was purified on RP-HPLC and characterized by ESI-MS. DNA linker **5** was assembled on automatic synthesizer using 1 μmol scale standard protocol and phosphoroamidite chemistry. After cleavage and deprotection, the oligomer was purified by HPLC on an anionic exchange column, desalted by gel filtration, and characterized by MALDI-TOF spectrometry. UV quantification of the purified PNA **4** and DNA **5** showed 10% and 59% yields, respectively.

We verified the effective formation of PNA/DNA duplex by CD measurements carried out in a tandem cell. Figure 5a shows the *sum* CD spectrum (solid line) of the two separated sample solutions (PNA tridendron in one compartment and DNA in the other one),

Journal of PeptideScience

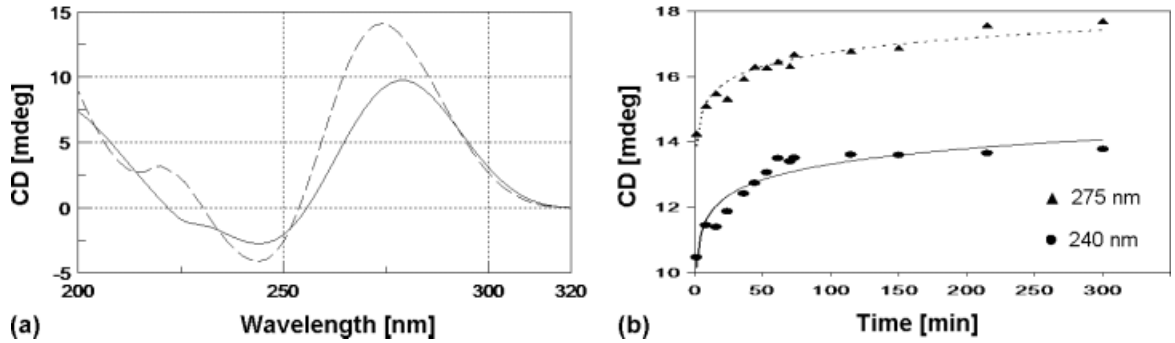

Figure 5. (a) Sum (solid line) and mix (dashed line) CD spectra of the 1 : 2.5 PNA/DNA complex (**4/5**, 4/10 μM), 20 °C in H_2O, pH 7.0 and (b) CD kinetic experiments on system **B**.

Linker (5) / Tridendron (4)	T_m ± 0.5 (°C)
1	38.8
1.5	41.6
2	42.8
2.5	40.3
3	37.0

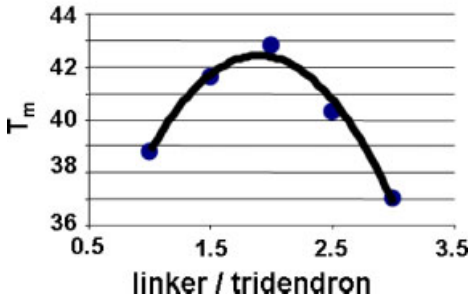

Figure 6. Table and bell curve of T_m values at the corresponding linker/tridendron concentration ratio. This figure is available in colour online at www.interscience.wiley.com/journal/jpepsci.

and the *mix* spectrum (dashed line) obtained after mixing the two samples (1 : 2.5 tridendron/linker ratio). We showed a significant difference between the two spectra, with an increase of intensity and a shift to lower wavelengths of the 280-nm band in the *mix* spectrum, clear evidence of duplex formation.

Furthermore, kinetic studies on complex formation in system **B** were performed by CD measurements, recording CD spectra at different times, after mixing the two strands. The CD value at 240 and 275 nm reported as a function of time reached a maximum and then remained stable, indicating the complete formation of complexes and hence of the supramolecular network, about 100 min after mixing PNA and DNA samples (Figure 5b).

We successively investigated, by UV melting studies, the optimum concentration ratio of the two components of system **B** (**4** and **5**) at which the most extensive polymeric network was formed. We expected to obtain the highest T_m in correspondence of the sample containing the most extensive network, as already reported by Shchepinov *et al*. [12]. The table contained in Figure 6 shows the T_m values at the corresponding linker (**5**)/tridendron (**4**) ratio, in UV experiments in which the tridendron concentration was fixed and the DNA linker concentration was gradually increased. A bell curve with a maximum at 2 was obtained by plotting the T_m *versus* concentration ratio (Figure 6). Thus, we concluded that to obtain the most extensive polymeric network, two DNA linker molecules for each PNA tridendron were required.

Microrheology Experiments

In order to evaluate the viscoelastic properties of systems **A** and **B**, microrheology experiments were performed by using the MPT technique.

A typical experimental MPT setup uses video microscopy to track the Brownian motion of micro-sized and nano-sized, inert, fluorescent particles embedded in samples [22,23]. Information about the local mechanical properties of the sample is then obtained by performing statistical analysis of the tracer particle motion.

The samples of the two systems were prepared by dissolving the lyophilized oligomers in 200 μl of water, heating at 90 °C for 5 min, slowly cooling at room temperature, and finally storing at 4 °C for 12 h. For system **A**, the experiments were performed using 50 and 200 μM concentrations of PNA **1** at 20 °C. For system **B**, we used the optimum concentration ratio of linker/tridendron (2 : 1) and 50 and 200 μM overall concentrations at 20 °C. Successively, a solution of fluorescent polystyrene beads (diameter 0.55 μm) was added to each sample solution and the resulting mixtures were fixed on glass slides and stored for 10 min at 4 °C to perform microrheology experiments. A set of images (8 fps) were collected using a CCD camera mounted on an inverted microscope. A computer calculated the number of beads and their position in the recorded image by using a two-dimensional particle tracking algorithm.

The results obtained were processed by an homemade Matlab program, allowing us to obtain the MSD and then, by the generalized Stokes–Einstein equation [24], the dynamic parameters G' and G''. G' and G'' characterize the elasticity (i.e. stiffness) and the viscous modulus of the investigated materials, respectively, [25]. From the experimental data analysis, we obtained the mechanical spectra (G' and G'' as function of frequency) for the noncovalent polymeric systems **A** and **B** (Figure 7). The spectra showed for both systems a viscous modulus higher than the elastic modulus ($G'' > G'$) in the entire frequency range (~0.1–10 Hz), exhibiting frequency profiles typical of dilute polymer solutions [26,27].

Therefore, the particle tracking measurements suggest that the analyzed samples behave like viscous liquids. The slope of the viscous modulus changes from close to 0.9 in the low-frequency regime to 0.7 at higher frequencies, indicating a change in the response of the sample from a viscous-like behavior to a comparatively more elastic-like behavior. This effect is attributable to the

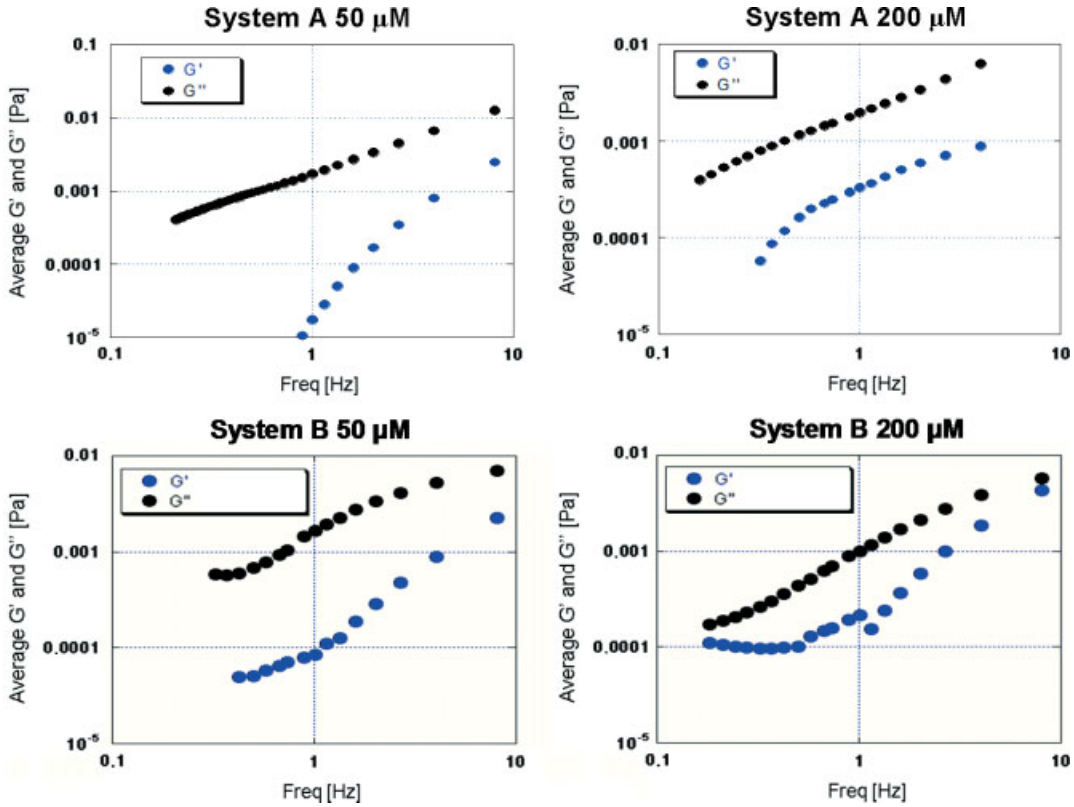

Figure 7. Microrheology data of systems **A** and **B**.

time dependence viscoelasticity of the material. At very long lag times, the polymer chains are free to diffuse around, which results in a more viscous-like response at low frequencies. However, at shorter times, these chains are constrained in their excursions, resulting in a more elastic-like behavior at high frequencies. The size of the fluorescent microbeads (550 nm) used for the particle tracking experiments, much larger than the molecular mesh size, ensure that mechanical spectra are strictly related to the polymer dynamics and completely decoupled by any solvent effect.

Because PNAs can aggregate at high concentrations, we performed, as control, microrheology experiments also on the a_5/t_5 (**2/3**) complex at the same concentrations used for PNA **1** (system **A**). In this case, a dependence of G' and G'' on the frequency typical of nonviscous liquids was observed (data not shown).

Conclusions and Perspectives

This work describes thermodynamic, kinetic, and microrheological studies on hyperbranched polymers based on PNA and DNA building blocks. We realized two kinds of systems: a PNA-based system (**A**, Figure 1) formed by a self-assembling PNA tridendron, and a PNA/DNA hybrid system (**B**, Figure 1) formed by a PNA tridendron and a DNA linker. The formation of a supramolecular network for both systems, by means of specific W-C base pairing, was investigated on the basis of detailed UV and CD spectroscopic studies. In particular, for the PNA-based system **A**, the intensity of the CD bands, the UV melting curve, and the PNA **1** concentration dependence of the T_m values were some features indicative of H-bond forming polymers. Furthermore, CD spectrum profile for **1** suggested a double helical PNA/PNA recognition, with a dominating left-handed helicity, at the basis of the supramolecular network. In the case of system **B**, kinetic CD data, together with the dependence of the T_m on the ratio of the PNA and DNA components, were in agreement with the hypothesized hyperbranched noncovalent polymer formation.

We successively performed microrheology experiments aimed to evaluate the viscoelastic properties of the systems, in view of their possible applications as nanomaterials sensitive to temperature or other external factors, as well as molecular delivery systems. These preliminary studies, performed by using the MPT technique, suggested for the analyzed samples a behavior typical of viscous liquids. This finding has important implications for the use of these polymeric systems in drug/gene delivery approaches or innovative environmental technologies such as the removal of pollutants from water: indeed the water solubility of the supramolecular networks is a fundamental characteristic in these kinds of applications. Moreover, we are currently exploring, by further spectroscopic and microrheological studies, whether these noncovalent polymeric systems form nanocavities of different dimensions and shape, able to encapsulate various bioactive pharmaceutical compounds or different water pollutants for the aforementioned applications.

References

1. Boas U, Heegaard PM. Dendrimers in drug research. *Chem. Soc. Rev.* 2004; **33**(1): 43–63.
2. Boas U, Christensen JB, Heegaard PMH. *Dendrimers in Medicine and Biotechnology: New Molecular Tools*. RSC Publishing: Cambridge, UK, 2006.
3. Lee CC, MacKay JA, Fréchet JM, Szoka FC. Designing dendrimers for biological applications. *Nat. Biotechnol.* 2005; **23**(12): 1517–1526.

4. Gillies ER, Fréchet JM. Dendrimers and dendritic polymers in drug delivery. *Drug Discov. Today* 2005; **10**(1): 35–43.
5. Svenson S, Tomalia DA. Dendrimers in biomedical applications-reflections on the field. *Adv. Drug Deliv. Rev.* 2005; **57**: 2106–2129.
6. Kobayashi H, James D, Kawamoto S, Brechbiel MW, Star RA, Choyke PL. Dendrimer-based nano-sized contrast agents for functional renal MRI: new insights into pathogenesis of acute renal diseases. *Contrast Media Mol. Imaging* 2005; **1**(2): 66–67.
7. Guillot-Nieckowski M, Eisler S, Diederich F. Dendritic vectors for gene transfection. *New J. Chem.* 2007; **31**: 1111–1127.
8. Arkas M, Allabashi R, Tsiourvas D, Mattausch E, Perfler R. Organic/inorganic hybrid filters based on dendritic and cyclodextrin "Nanosponges" for the removal of organic pollutants from water. *Environ. Sci. Technol.* 2006; **40**(8): 2771–2777.
9. Song C, Koo B, Kim C. Application of dendrimer as a new material for electrical and optical devices. *Jpn. J. Appl. Phys.* 2002; **41**: 2735–2738.
10. Li Y, Tseng YD, Kwon SY, D'Espaux L, Bunch JS, Mceuen PL, Luo D. Controlled assembly of dendrimer-like DNA. *Nat. Mater.* 2004; **3**: 38–42.
11. Luo D. The road from biology to materials. *Mater. Today* 2003; **6**(11): 38–43.
12. Shchepinov MS, Mir KU, Elder JK, Frank-Kamenetskii MD, Southern EM. Oligonucleotide dendrimers: stable nano-structures. *Nucleic Acids Res.* 1999; **27**(15): 3035–3041.
13. Luo D, Li Y, Um SH, Cu Y. A dendrimer-like DNA-based vector for dna delivery: a viral and nonviral hybrid approach. *Methods Mol. Med.* 2006; **127**: 115–126.
14. Biondi M, Ungaro F, Quaglia F, Netti PA. Controlled drug delivery in tissue engineering. *Adv. Drug Deliv. Rev.* 2008; **60**: 229–242.
15. Hamad-Schifferli K, Schwartz JJ, Santos AT, Zhang S, Jacobson JM. Remote electronic control of DNA hybridization through inductive coupling to an attached metal nanocrystal antenna. *Nature* 2002; **415**: 152–155.
16. Uhlmann E, Peyman A, Breipohl G, Will DW. Synthetic polyamide nucleic acids with unusual binding properties. *Angew. Chem. Int. Ed. Engl.* 1998; **37**: 2796–2823.
17. Silvester NC, Bushell GR, Searles DJ, Brown CL. Effect of terminal amino acids on the stability and specificity of PNA–DNA hybridization. *Org. Biomol. Chem.* 2007; **5**(6): 917–923.
18. Wittung P, Eriksson M, Lyng R, Nielsen PE, Nordén B. Induced chirality in PNA–PNA duplexes. *J. Am. Chem. Soc.* 1995; **117**: 10167–10173.
19. Wittung P, Nielsen PE, Norden B. Observation of a PNA/PNA/PNA triplex. *J. Am. Chem. Soc.* 1997; **119**: 3189–3190.
20. Lagriffoule P, Wittung P, Eriksson M, Jensen KK, Norden B, Buchardt O, Nielsen PE. PNAs with a conformationally constrained chiral cyclohexyl derived backbone. *Chem. Eur. J.* 1997; **3**(6): 912–919.
21. Tedeschi T, Sforza S, Dossena A, Corradini R, Marchelli R. Lysine-based peptide nucleic acids (PNAs) with strong chiral constraint: control of helix handedness and DNA binding by chirality. *Chirality* 2005; **17**: S196–S204.
22. Gardel ML, Valentine MT, Weitz DA. In *Microscale Diagnostic Techniques*, Brues KS (ed.). Springer: New York, 2005.
23. Mukhopadhyay A, Granick S. Micro- and nanorheology. *Curr. Opin. Colloid Interface Sci.* 2001; **6**: 423–429.
24. Waigh TA. Microrheology of complex fluids. *Rep. Prog. Phys.* 2005; **68**: 685–742.
25. Ferry J. *Viscoelastic Properties of Polymers*. John Wiley and Sons: New York, 1980.
26. Rouse PE. A theory of the linear viscoelastic properties of dilute solutions of coiling polymers. *J. Chem. Phys.* 1953; **21**: 1272–1280.
27. Zimm BH. Dynamics of polymer molecules in dilute solution: viscoelasticity, flow birefringence and dielectric loss. *J. Chem. Phys.* 1956; **24**: 269–278.

